Mizuguchi, N. Utsonomiya, M. Nakanishi, Y. Arata, *J. Immunol.* **140**, 2495 (1988).
8. The rabbit polyclonal antibodies to Vav used in this study include antibodies to a synthetic peptide corresponding to residues 576 to 589 of mouse $p95^{vav}$, a bacterial MBP fusion protein containing the cysteine-rich zinc finger–like region of mouse $p95^{vav}$ (residues 460 to 626), and a bacterial MBP fusion protein containing the HLH–leucine-rich region of mouse $p95^{vav}$ (residues 9 to 135).
9. M. R. Gold, D. A. Law, A. L. DeFranco, *Nature* **345**, 810 (1990); M. Brunswick, L. E. Samelson, J. J. Mond, *Proc. Natl. Acad. Sci. U.S.A.* **88**, 1311 (1991).
10. M. A. Campbell and B. M. Sefton, *EMBO J.* **9**, 2125 (1990).
11. Sequences encoding the murine $p95^{vav}$ SH2 domain (residues 659 to 773) were amplified by the polymerase chain reaction (PCR) with the pJC11 plasmid (*3*) as template and subcloned into the pMAL-c (NE Biolabs) or the pGEX-2T (Pharmacia) expression vectors. Cultures of *Escherichia coli* DHα cells transformed with pMAL-c expression plasmids containing the MBP fused to either the LacZ gene (β-gal) or the SH2 domain of $p95^{vav}$ were processed as suggested by the manufacturer. The MBP fusion proteins were purified by affinity chromatography with an amylose matrix and eluted in RIPA buffer containing maltose (10 mM). After elution, fusion proteins were immobilized on protein A–Sepharose beads (Pharmacia) coated with antibodies to MBP (NE Biolabs). Cultures of *E. coli* DHα containing the pGEX-2T plasmid encoding either the glutathione S-transferase (GST) protein alone or the GST-VavSH2 fusion protein were induced following standard protocols, and expressed proteins were purified with glutathione-Sepharose beads (Pharmacia). These beads were incubated directly with cellular lysates. In binding experiments, cells were lysed by adding into the medium 1/5 volume of 5× RIPA buffer containing phosphatase inhibitors. Lysates were mixed with Sepharose beads containing the appropriate bacterial MBP fusion protein by gentle inversion for 3 hours at 4°C. Complexes were recovered by centrifugation, washed, and eluted with SDS-PAGE sample buffer.
12. Y. Yamanashi, T. Kakiuchi, J. Mizuguchi, T. Yamamoto, K. Toyoshima, *Science* **251**, 192 (1991); A. L. Burkhardt, M. Brunswick, J. B. Bolen, J. J. Mond, *Proc. Natl. Acad. Sci. U.S.A.* **88**, 7410 (1991).
13. J. E. Hutchcroft, M. L. Harrison, R. L. Geahlen, *J. Biol. Chem.* **266**, 14846 (1991).
14. X. R. Bustelo and M. Barbacid, unpublished observations.
15. J. E. Coligan, A. M. Kruisbeek, D. H. Margulies, E. M. Shevach, W. Strouber, *Current Protocols in Immunology* (Wiley Interscience, New York, 1991), chap. 3.
16. We thank A. Burkhardt and J. Bolen for providing the WEHI-231 and Bal17 B cell lines and K. L. Suen for generating the plasmid encoding the GST-VavSH2 fusion protein. X.R.B. was supported by a postdoctoral fellowship from the Spanish Ministerio de Educación y Ciencia.

29 January 1992; accepted 16 April 1992

Calmodulin Trapping by Calcium-Calmodulin–Dependent Protein Kinase

Tobias Meyer,* Phyllis I. Hanson, Lubert Stryer, Howard Schulman†

Multifunctional calcium-calmodulin–dependent protein kinase (CaM kinase) transduces transient elevations in intracellular calcium into changes in the phosphorylation state and activity of target proteins. By fluorescence emission anisotropy, the affinity of CaM kinase for dansylated calmodulin was measured and found to increase 1000 times after autophosphorylation of the threonine at position 286 of the protein. Autophosphorylation markedly slowed the release of bound calcium-calmodulin; the release time increased from less than a second to several hundred seconds. In essence, calmodulin is trapped by autophosphorylation. The shift in affinity does not occur in a site-directed mutant in which threonine at position 286 has been replaced by a non-phosphorylatable amino acid. These experiments demonstrate the existence of a new state in which calmodulin is bound to CaM kinase even though the concentration of calcium is basal. Calmodulin trapping provides for molecular potentiation of calcium transients and may enable detection of their frequency.

Multifunctional CaM kinase is a ubiquitous mediator of Ca^{2+} effects in neurotransmission, neuronal plasticity, ion channels, and carbohydrate metabolism (*1*). CaM kinase constitutes up to 1% of total brain protein and 2% of hippocampal protein, and its concentration in synaptic spines is roughly comparable to that of total calmodulin (*2*). Neuronal CaM kinase consists of α (54 kD) and β or β′ (60 or 58 kD) subunits in ~10 subunit multimers. Each isoform has a catalytic domain, a regulatory domain consisting of an autoinhibitory and a calmodulin-binding region, and an association (oligomerization) domain. Each subunit of the kinase becomes activated when Ca^{2+}-calmodulin binds to and displaces the autoinhibitory domain from its active site. The activated kinase further disrupts the interaction of the autoinhibitory region with the catalytic site by phosphorylating Thr^{286} and Thr^{287} of the α and β subunits, respectively. After dissociation of calmodulin from an autophosphorylated CaM kinase, the modified subunit remains partially active (termed autonomous). Subsequent Ca^{2+}-independent autophosphorylation occurs within the vacated calmodulin-binding region; these phosphorylated residues are termed inhibitory sites because their modification blocks the binding of calmodulin and thereby prevents maximal activation.

We have investigated the effect of autophosphorylation of CaM kinase on binding and release of calmodulin by the technique of fluorescence emission anisotropy (*3*) with dansylated calmodulin (CaM^F) as a probe (*4*). The rotational mobility of CaM^F can be assessed by exciting with vertically polarized light and measuring differences in emission of vertically (F_V) and horizontally (F_H) polarized light. The emission anisotropy is defined as $A = (F_V - F_H)/(F_V + 2F_H)$. The value of A increases when calmodulin (17 kD) binds to CaM kinase (~600 kD) because the rotational mobility of the fluorescent probe is markedly decreased. The binding of Ca^{2+} to CaM^F in the absence of CaM kinase resulted in a small decrease in anisotropy (Fig. 1). Subsequent addition of purified rat brain CaM kinase (*5*) in the absence of adenosine triphosphate (ATP) led to a large increase

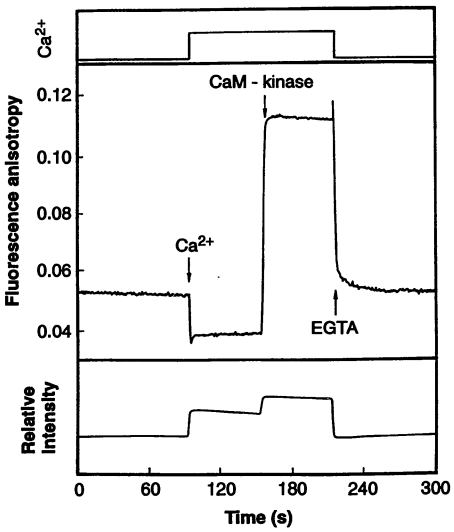

Fig. 1. Time course of binding and release of dansylated CaM from CaM kinase. The buffer solution contained 5 mM Mg^{2+}, 50 mM potassium acetate, and 15 mM Hepes (pH 7, adjusted with KOH). Increasing the free Ca^{2+} concentration from 100 nM to 200 μM decreases the fluorescence anisotropy of CaM^F (20 nM) slightly from 0.054 to 0.040. Addition of an excess of CaM kinase (60 nM binding sites) markedly increases the fluorescence anisotropy to 0.12. This increase is due to the binding of CaM^F to the large CaM kinase oligomer. When the free Ca^{2+} concentration is lowered to less than 100 nM by addition of 3 mM EGTA, the fluorescence anisotropy drops rapidly to 0.054, the value characteristic of free CaM^F without bound Ca^{2+}.

T. Meyer and L. Stryer, Department of Cell Biology, Stanford University School of Medicine, Stanford, CA 94305.
P. I. Hanson and H. Schulman, Department of Pharmacology, Stanford University School of Medicine, Stanford, CA 94305.

*Present address: Department of Cell Biology, Duke University Medical Center, Durham, NC 27710.
†To whom correspondence should be addressed.

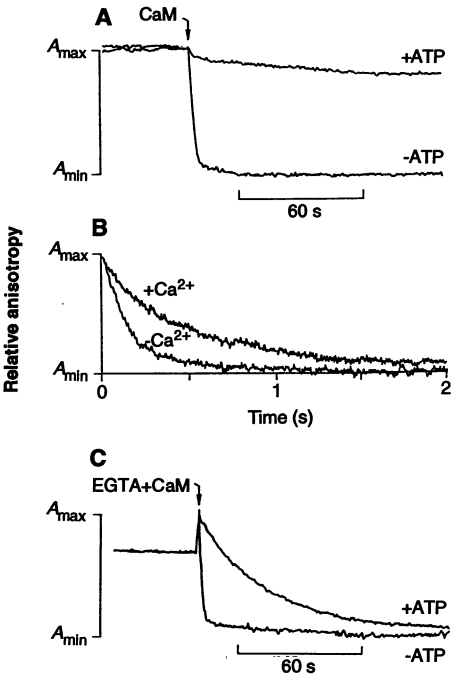

Fig. 2. Dissociation kinetics of CaM^F in the presence and absence of ATP. (**A**) Release of CaM^F (20 nM) after the addition of an excess of unlabeled CaM (~300 nM). Ca^{2+} (50 μM), CaM^F, and CaM kinase (18 nM binding sites) were preincubated with or without ATP (+ATP or −ATP) for 60 s. A_{min} is the anisotropy level before kinase addition. (**B**) Rapid mixing studies to resolve the subsecond CaM^F dissociation kinetics in the absence of ATP were performed by filling one syringe with 50 μM Ca^{2+}, 100 nM CaM^F, and 120 nM CaM kinase and the other one with either 2 mM EGTA or 50 μM Ca^{2+} and 2 μM unlabeled CaM. Data are the average of 12 experiments performed with the same instrument and a Hi-Tech SFA-II stop-flow device. In these measurements, the integration time of the signal was 25 ms. (**C**) Release of bound CaM^F on lowering free Ca^{2+} to 200 nM (in combination with an excess of CaM). A_{min} is here the steady-state anisotropy after addition of Ca^{2+} and EGTA. For these experiments, the maximal anisotropy level (A_{max}) is defined relative to the final anisotropy level (A_{min}): $A_{max} = A_{min} + \Delta A$. This is because the addition of EGTA leads to a slight increase of the anisotropy of unbound CaM^F (Fig. 1). ΔA is determined from the initial anisotropy difference when kinase was added to Ca^{2+}-CaM^F.

in anisotropy, which is indicative of the binding of CaM^F to the oligomeric CaM kinase. Addition of EGTA to lower the free Ca^{2+} concentration to less than 100 nM (6) led to the dissociation of CaM, as shown by the reversal of the increase in anisotropy.

How is the rate of calmodulin dissociation affected by exposure to ATP? Incubation of CaM kinase with Ca^{2+}-CaM^F and ATP leads to the virtually irreversible binding of calmodulin (Fig. 2A). At high Ca^{2+} concentration, labeled CaM^F does not substantially exchange for unlabeled calmodulin in hundreds of seconds. In the absence of ATP, however, the exchange rate is rapid and can be resolved in stopped-flow measurements (Fig. 2B). CaM^F exchanges for unlabeled calmodulin in 460 ms (63% exchanged). CaM^F is also rapidly released when the free Ca^{2+} concentration is lowered by the addition of EGTA (Fig. 1). CaM^F then dissociates in 170 ms (Fig. 2B). CaM kinase that has been preincubated with ATP also releases CaM^F slowly when Ca^{2+} concentrations are decreased. At 200 nM free Ca^{2+}, CaM^F dissociates in 20 s (Fig. 2C). We measured the dependence of the dissociation time for calmodulin for samples that were previously incubated either with or without ATP at a high Ca^{2+} concentration. Prior exposure to ATP increases the dissociation time of calmodulin 100- to 1000-fold, depending on the final Ca^{2+} concentration. In the absence of ATP, the dissociation time of calmodulin is much faster and depends only slightly on the final Ca^{2+} concentration. Thus, calmodulin cannot dissociate from kinase that was incubated with ATP unless the Ca^{2+} concentration drops back to basal (~100 nM) for at least 10 s (Fig. 3). At higher Ca^{2+} concentrations or in shorter times, calmodulin remains trapped.

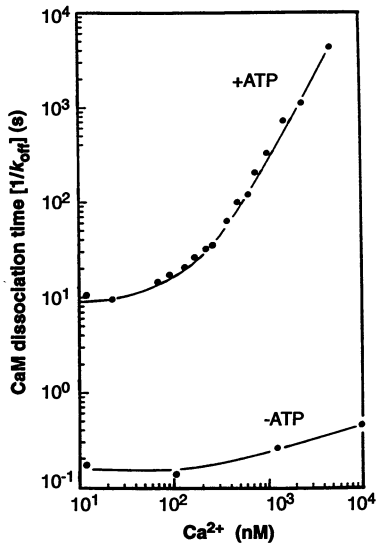

Fig. 3. Ca^{2+} dependence of the dissociation time of CaM^F from its complex with the kinase. Dissociation kinetics were measured in experiments similar to those in Fig. 2C after the combined addition of 300 nM unlabeled CaM and various Ca^{2+}/EGTA ratios (2 mM final EGTA) to CaM^F (20 nM) and kinase (18 nM sites). The inclusion of 300 nM unlabeled calmodulin increases the amount of released CaM^F at intermediate Ca^{2+} concentrations. The time constants on the *y* axis correspond to the times required for dissociation of 63% of bound CaM^F ($1/k_{off}$). The upper curve gives the dissociation times following preincubation with ATP. The lower curve gives the dissociation times in the absence of ATP. These data points were measured by rapid-mixing as described in Fig. 2B.

Table 1. Binding of dansylated calmodulin to α-CaM kinase.

α-CaM kinase		$1/k_{off}$ (s)	k_{on} (M^{-1} s^{-1})	K_d (nM)
Unphosphorylated	$+Ca^{2+}$	0.46	1.5×10^8	14.5
	$-Ca^{2+}$	0.17		
Phosphorylated at Thr^{286}	$+Ca^{2+}$	>1000	0.5×10^8	<0.02
	$-Ca^{2+}$	10		

The same kinetic method enabled us to measure the rate at which CaM^F bound to ATP-treated and untreated CaM kinase and thereby to deduce the dissociation constants of the complexes. On-rate constants were about 0.5×10^8 M^{-1} s^{-1} after incubation with ATP and 1.5×10^8 M^{-1} s^{-1} without ATP (*7*). Hence, the affinity of CaM^F increases about 1000-fold after exposure to ATP, from 15 nM to less than 20 pM (Table 1). Competitive binding studies demonstrated that trapping is not confined to dansylated calmodulin and that unlabeled calmodulin can also be trapped (*8*).

Is the trapping of calmodulin caused by the binding of ATP or by the consequent autophosphorylation of the kinase? Trapping cannot be induced by incubation with adenosine β, γ-imidoadenosine-5′-triphosphate, a hydrolysis-resistant analog of ATP. Once trapped, calmodulin remains bound when ATP is rapidly depleted by addition of hexokinase and glucose (*9*). This implies that a persistent ATP-mediated modifica-

Table 2. Dissociation constants of complexes between Ca^{2+}-calmodulin and target proteins (*17*).

Target proteins	K_d (nM)
Neuromodulin*	100
CaM kinase, unphosphorylated†	45
Phosphorylase kinase‡	20
Adenylate cyclase	15
Calcineurin	6
Ca^{2+}-ATPase pump (plasma membrane)	5
MARCKS	2.8
Myosin light chain kinase (smooth muscle)	1
Cyclic AMP phosphodiesterase	0.1
CaM kinase, autonomous	0.06

*This affinity is independent of calcium level. †The threefold lower affinity of α-CaM kinase for calmodulin is shown instead of the one for CaM^F. It is assumed that the shift in K_d between calmodulin and CaM^F is similar for phosphorylated and unphosphorylated CaM kinase. ‡Two calmodulin are needed for maximal activation, the first calmodulin is a subunit of phosphorylase kinase.

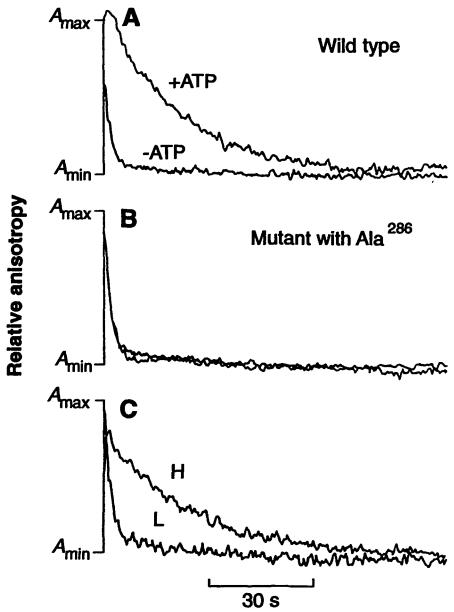

Fig. 4. Trapping of CaM^F by recombinant CaM kinase. (**A**) Wild-type α-CaM kinase (~12 nM sites) was preincubated for 30 s with 15 nM CaM^F either with 200 μM ATP (+ATP) or without ATP (−ATP). The free Ca^{2+} concentration was then lowered from 200 μM to 100 nM by addition of EGTA to initiate dissociation. (**B**) Mutant kinase containing Ala^{286} instead of Thr^{286} was preincubated with or without ATP trapping and examined as above. (**C**) α-CaM kinase (1-326), a monomeric CaM kinase expressed in COS-7 cells and purified, autophosphorylates its autonomy site during a preincubation with ATP only at a high monomer concentration. Trapping exhibits a similar concentration dependence. There is little trapping following a 30-s preincubation of monomeric α-CaM kinase (1-326) at a low concentration (~12 nM) (L). Almost complete trapping does occur after a similar preincubation of monomer at a high concentration (~200 nM sites) for 2 min (H).

tion is necessary for trapping. A candidate for this process is autophosphorylation of the autonomy site (Thr^{286} on α-CaM kinase) (*10*, *11*).

Site-directed mutants of CaM kinase were used to test this hypothesis. Recombinant wild-type CaM kinase (α isoform) purified from transfected COS cells (*12*) shows virtually the same ATP-mediated trapping as does CaM kinase purified from brain kinase (Fig. 4A). Mutants in which Thr^{286} is replaced by an amino acid that cannot be phosphorylated, such as alanine (Ala^{286} α-CaM kinase), have wild-type levels of Ca^{2+}-stimulated activity toward exogenous substrates but do not exhibit Ca^{2+}-independent activity (*12*, *13*). Trapping is not observed in the Ala^{286} α-CaM kinase mutant (Fig. 4B). Phosphorylation of the autonomy site is therefore necessary for calmodulin trapping. Does trapping depend on the oligomeric structure of CaM kinase, or might a phosphorylated monomer suffice? A monomeric α-CaM kinase was generated by deleting the oligomerization domain (*14*). Figure 4C demonstrates that the phosphorylated monomeric mutant can trap calmodulin. Hence, each of the eight to ten calmodulin traps of a multimer is controlled by whether its own autonomy site is phosphorylated.

Autophosphorylation of Thr^{286} has been shown to confer partial activity on CaM kinase in the absence of bound Ca^{2+}-calmodulin (*11–13*, *15*). The presence of a phosphate moiety within the autoinhibitory domain of the kinase allows it to maintain activity even when stripped of calmodulin. Here we show that autophosphorylation also markedly increases the affinity of CaM kinase for calmodulin. The dissociation of calmodulin from CaM kinase after a decrease in the concentration of Ca^{2+} is more than 100-fold slower for the phosphorylated than for the unphosphorylated enzyme. Is this slowed dissociation reflected in prolonged calmodulin-stimulated kinase activity after chelation of Ca^{2+} from the autophosphorylated kinase? Without autophosphorylation, CaM kinase is rapidly deactivated when the Ca^{2+} concentration is decreased to 10 nM. Average kinase activity measured during the first 10 s after chelation of Ca^{2+} drops from the stimulated level of 100% to 5.5 ± 0.8% (n = 4). By contrast, activity remains at 85 ± 8% (n = 6) of maximal during the first 10 s if Ca^{2+} is lowered after autophosphorylation has occurred. Activity in this trapped state is higher than the autonomous activity (activity of the autophosphorylated kinase after complete dissociation of CaM^F), which under these conditions was 38 ± 6% (n = 4).

These experimental data demonstrate the existence of a new state in which CaM stays bound even though the Ca^{2+} level has returned to baseline. This new state is likely to be biologically significant for several reasons: (i) Trapping allows the kinase to maintain full activity for many seconds after Ca^{2+} declines to basal levels. This mechanism may be of particular importance in the potentiation of brief (<1 s) Ca^{2+} transients. (ii) Many systems respond to hormonal stimuli with an initial rapid rise in Ca^{2+} that is followed by a longer period in which Ca^{2+} declines to a plateau level that is higher than basal. Under these circumstances, kinase activity would be prolonged even further, because at intermediate Ca^{2+} concentrations calmodulin is trapped for tens of seconds (Fig. 3). (iii) Finally, calmodulin trapping masks the inhibitory phosphorylation site and thus delays the formation of an enzyme that is refractory to further stimulation by Ca^{2+}-calmodulin.

A new consequence of trapping would come into play if calmodulin is limiting (*16*). This condition could result from Ca^{2+} concentrations that do not saturate calmodulin, from Ca^{2+} pulses that are too short to permit the attainment of equilibrium, or from calmodulin concentrations that are locally lower than the concentration of calmodulin-binding sites. It is revealing to compare the affinity of dephosphorylated and phosphorylated CaM kinase for Ca^{2+}-calmodulin with that of other calmodulin-binding proteins (Table 2). Dephosphorylated CaM kinase has one of the lowest affinities for calmodulin, whereas CaM kinase phosphorylated at the autonomy site has the highest. How might nature exploit this large shift in affinity? Consider a calcium spike that elicits only partial occupancy of the calmodulin-binding sites of CaM kinase and hence submaximal activation of the kinase. As Ca^{2+} declines, autophosphorylated subunits transit through a highly active trapped state and then a less active calmodulin-free autonomous state before dephosphorylation and return to the basal state. At a low frequency of stimulation, each Ca^{2+} spike would produce the same submaximal activation of CaM kinase. If the frequency of Ca^{2+} transients is high, however, trapped calmodulin will not significantly dissociate between spikes. At each successive spike, the kinase will recruit additional calmodulin molecules that dissociate from other calmodulin-binding proteins and thereby become increasingly activated. Thus trapping, in addition to potentiating brief repetitive Ca^{2+} signals, may enable the kinase to detect their frequency.

REFERENCES AND NOTES

1. P. I. Hanson and H. Schulman, *Annu. Rev. Biochem.* **61**, 559 (1992); H. Schulman, *Curr. Opin. Neurobiol.* **1**, 43 (1991); R. J. Colbran and T. R. Soderling, *Curr. Top. Cell. Regul.* **31**, 181 (1989). CaM kinase is also referred to as Ca^{2+}-calmodulin–dependent multiprotein kinase, type II Ca^{2+}-calmodulin–dependent protein kinase, and Ca^{2+}-calmodulin–dependent protein kinase II.
2. N. E. Erondu and M. B. Kennedy, *J. Neurosci.* **5**, 3270 (1985); M. B. Kennedy *et al.*, *Cold Spring Harbor Symp. Quant. Biol.* **LV**, 101 (1990); S. S. Molloy and M. B. Kennedy, *Proc. Natl. Acad. Sci. U.S.A.* **88**, 4756 (1991).
3. Fluorescence anisotropy was measured with a custom-made instrument that uses the 335-nm line of an Oriel mercury lamp (Stratford, CT), a Schoeffel Instruments single monochromator grating, an excitation polarizer that can be rotated 90°C for calibration purposes, and an additional block filter at 400 nm to suppress any light of higher wavelength that may have passed through the monochromator. The vertically polarized excitation beam was focused on a 1-cm, temperature-controlled, stirred quartz cuvette with a 2-s mixing time. The experiments were performed at 30°C. The parallel and perpendicular components of the emitted light were measured with two fixed polarizers and photomultiplier tubes. Excitation light below 500 nm was suppressed with emission cutoff filters. The signals from the reference and the two fluorescence photomultiplier tubes were amplified and integrated for 1 s. The data points were then collected with a Metrabyte Das8 board (Taunton, MA) and a 286 personal computer. The intensity and fluorescence anisotropy of the signal

were determined as $I_{tot} = C(F_V - B_V) + 2(F_H - B_H)$, $A_n = [C(F_V - B_V) - (F_H - B_H)]/I_{tot}$. Abbreviations: I_{tot}, total relative intensity; C, calibration ratio from the horizontal to the vertical fluorescence channel; F_V and F_H, vertical and horizontal polarized fluorescence signals, respectively; B_V and B_H, vertical and horizontal polarized background, respectively; A_n, resulting anisotropy. The calibration factor (C) and the background light (B_V and B_H) were determined before each experiment.

4. Randomly dansylated calmodulin has been used for calmodulin-binding studies [reviewed in R. L. Kincaid, M. L. Billingsley, M. Vaughn, *Methods Enzymol.* **159**, 605 (1988)]. For the present experiments, differentially labeled forms of dansylated calmodulin were separated from such a random pool. Calmodulin (Ocean Biologics, Edmonds, WA) was incubated with an approximately fourfold molar excess of dansyl chloride for 45 min at room temperature (10 mg of calmodulin per milliliter, pH 9.0, 50 mM KCl, 20 mM Hepes). Unreacted dansyl was then separated from dansylated calmodulin on a Sephadex G50 column (Piscataway, NJ). Calmodulin species with different amounts of labeling were separated on a high-pressure liquid chromatography hydrophobic interaction column (MP7, Bio-Rad, Richmond, CA) in an ammonium sulfate gradient (1.5 M to 0 M; 100 mM phosphate present in both buffers, pH 7.0). The first peak, which eluted after unlabeled CaM, was designated as CaM^F and used for all studies. Competitive binding studies demonstrated that the affinity of unlabeled calmodulin for CaM kinase is approximately threefold lower than that of CaM^F. The concentration of CaM^F was determined by quantitative amino acid analysis. The concentration of CaM kinase subunits was defined by the concentration of calmodulin binding sites in the preparation.
5. A large amount of rat forebrain CaM kinase (5 mg) was obtained by a three-step purification procedure [H. Schulman, *J. Cell Biol.* **99**, 11 (1984)]. Most of the experiments were repeated with CaM kinase from two separate preparations with similar results.
6. The free Ca^{2+} concentration was initially estimated from Ca^{2+}/EGTA ratios and then determined fluorometrically with the calcium indicator rho-2 [dissociation constant (K_D)-1.0 μM] [A. Minta, J. P. Kao, R. Y. Tsien, *J. Biol. Chem.* **264**, 8171 (1990)].
7. The on-rate of CaM^F to CaM kinase in the absence of ATP was determined by the addition of EGTA and then Ca^{2+} to a highly diluted sample (1.25 nM CaM^F and 1.5 nM CaM kinase subunits). The on-rate was estimated from the time it took for rebinding. The on-rate for CaM^F binding to ATP-exposed CaM kinase was determined by the incubation of high concentrations of CaM^F and CaM kinase subunits (500 nM) in the presence of ATP for 15 s. After this period, glucose (10 mM) and hexokinase (2 U/ml) were added, and then the sample was diluted into the cuvette (final concentrations approximately 5 nM). EGTA was added, and CaM^F was allowed to dissociate for 40 s. The addition of an excess of Ca^{2+} led to the rebinding of CaM^F. The on-rates given in the text are averages of three experiments.
8. Competitive binding studies show that CaM^F has a threefold higher affinity for unphosphorylated CaM kinase than does unlabeled calmodulin. When unlabeled calmodulin is trapped at high Ca^{2+} concentrations in the presence of ATP, it cannot be replaced with CaM^F for long periods of time, indicating that unlabeled CaM, like CaM^F, can be trapped.
9. T. Meyer and L. Stryer, *Proc. Natl. Acad. Sci. U.S.A.* **87**, 3841 (1990).
10. Y. Lai, A. C. Nairn, F. Gorelick, P. Greengard, *ibid.* **84**, 5710 (1987); C. M. Schworer, R. J. Colbran, J. R. Keefer, T. R. Soderling, *J. Biol. Chem.* **263**, 13486 (1988); L. L. Lou and H. Schulman, *J. Neurosci.* **9**, 2020 (1989).
11. S. G. Miller, B. L. Patton, M. B. Kennedy, *Neuron* **1**, 593 (1988).
12. The SRα expression vectors encoding α-CaM kinase or mutant CaM kinase were transfected into COS-7 cells [P. I. Hanson, M. S. Kapiloff, L. L. Lou, M. G. Rosenfeld, H. Schulman, *ibid.* **3**, 59 (1989)]. CaM kinase was purified by chromatography on DE-52, phosphocellulose, and calmodulin-Sepharose (*5*).
13. Y. L. Fong, W. L. Taylor, A. R. Means, T. R. Soderling, *J. Biol. Chem.* **264**, 16759 (1989). The Ala^{286} replacement was generated with a 23–base pair oligonucleotide (5′-GGC AGT CCA CGG CCT CCT GTCTG-3′) by standard procedures.
14. T. Yamauchi, S. Ohsaka, T. Deguchi, *ibid.*, p. 19108.
15. G. Thiel, A. J. Czernik, F. Gorelick, A. C. Nairn, P. Greengard, *Proc. Natl. Acad. Sci. U.S.A.* **85**, 6337 (1988).
16. R. P. Estep, K. A. Alexander, D. R. Storm, *Curr. Top. Cell. Regul.* **31**, 161 (1989); J. H. P. Skene, *Neurosci. Res. Suppl.* **13**, S112 (1990).
17. Binding data (or $K_{1/2}$ for activation, if binding data are not available) are from *Calmodulin*, P. Cohen and C. B. Klee, Eds. (Elsevier, Amsterdam, 1988); value for MARCKS was determined from peptide binding, J. M. Graff, T. N. Young, J. D. Johnson, P. J. Blackshear, *J. Biol. Chem.* **264**, 21818 (1989); data for the nonbacterial cyclase are from G. B. Rosenberg, A. V. M. Minocherhomjee, D. R. Storm, *Methods Enzymol.* **139**, 776 (1987).
18. Supported by GM24032 and MH45324 to L.S., GM 40600 to H.S., PHS training grant CA09302 to P.I.H., and a Swiss National Science Foundation fellowship to T.M.

4 November 1991; accepted 11 March 1992

A Mutant of TTX-Resistant Cardiac Sodium Channels with TTX-Sensitive Properties

Jonathan Satin,* John W. Kyle, Michael Chen, Peter Bell, Leanne L. Cribbs, Harry A. Fozzard, Richard B. Rogart

The cardiac sodium channel α subunit (RHI) is less sensitive to tetrodotoxin (TTX) and saxitoxin (STX) and more sensitive to cadmium than brain and skeletal muscle (μI) isoforms. An RHI mutant, with Tyr substituted for Cys at position 374 (as in μI) confers three properties of TTX-sensitive channels: (i) greater sensitivity to TTX (730-fold); (ii) lower sensitivity to cadmium (28-fold); and (iii) altered additional block by toxin upon repetitive stimulation. Thus, the primary determinant of high-affinity TTX-STX binding is a critical aromatic residue at position 374, and the interaction may take place possibly through an ionized hydrogen bond. This finding requires revision of the sodium channel pore structure that has been previously suggested by homology with the potassium channel.

Two classes of Na^+ channel subtypes (*1*) have been distinguished by their sensitivity to TTX and STX. Sodium channels in brain and innervated skeletal muscles that are TTX-sensitive (TTX-S) are blocked by nanomolar concentrations of TTX (*2*), whereas TTX-resistant (TTX-R) Na^+ channels in heart and denervated skeletal muscle are blocked by micromolar concentrations of TTX (*3*, *4*). Molecular cloning and expression of Na^+ channel cDNAs show multiple isoforms of Na^+ channels that are encoded by a multigene family in mammals (*5*), where a difference in primary structure accounts for the possession of TTX-S or TTX-R properties (*6*, *7*).

Molecular studies have provided information that locates the structural domain where TTX and STX bind to and block the Na^+ channel, thereby identifying the external entrance to the channel pore. The SS2 domain (Fig. 1) is a seven–amino acid segment that forms part of the external loop that connects membrane-spanning units S5 and S6. In the Brain II Na^+ channel, substitution of Glu^{387} with Gln in SS2 of the first (NH_2-terminal) repeat abolished sensitivity to TTX and STX (*8*, *9*). In K^+ channels, mutagenesis of a region analogous to SS1 and SS2 (Fig. 1) modifies pore properties, including sensitivity to external blocking agents acting like TTX and STX (*10*).

Two of the seven amino acids in SS2 of the first NH_2-terminal repeat differ between the RHI (*11*) and the TTX-S Na^+ channel isoforms (Fig. 1). We mutated these two positions (*12*) to the corresponding amino acids found in the TTX-S skeletal muscle Na^+ channel isoform (μI). We determined the TTX and STX sensitivity for the RHI $Arg^{377} \rightarrow$ Asn mutant, where substitution of the positively charged Arg with a neutral Asn was predicted to restore TTX and STX sensitivity to the RHI Na^+ channel (*8*). The Na^+ current (I_{Na}) was elicited by a 7-ms depolarization to −10 mV in the presence of various concentrations of TTX (Fig. 2). Single-site dose-response curves for blockage of I_{Na} by toxin for the wild-type RHI and the $Arg^{377} \rightarrow$ Asn mutant are best fit with apparent dissociation constants (K_d) for TTX of 0.95 μM and 7.58 μM, respectively (Fig. 3A); the K_d's for STX are 91 nM and 184 nM, respectively. Thus, the

J. Satin and H. A. Fozzard, Laboratory of Cardiac Electrophysiology, Departments of Medicine and Pharmacological and Physiological Sciences, and The Committee on Cell Physiology, The University of Chicago, MC-6094, 5841 South Maryland Avenue, Chicago, IL 60637.
J. W. Kyle, M. Chen, P. Bell, L. L. Cribbs, R. B. Rogart, Laboratory of Molecular Neuro-Cardiology, Department of Medicine, and The Committee on Cell Physiology, The University of Chicago, MC-6094, 5841 South Maryland Avenue, Chicago, IL 60637.
*To whom correspondence should be addressed.